EFDA–JET–CP(12)02/18

J. Miettunena, M. Groth, T. Kurki-Suonio, H. Bergsåker, J. Likonen,
S. Marsen, C. Silva, S. Äkäslompolo and JET EFDA contributors

Predictive ASCOT Modelling of ^{10}Be Transport in JET with the ITER-Like Wall

Predictive ASCOT Modelling of ^{10}Be Transport in JET with the ITER-Like Wall

J. Miettunen[1], M. Groth[1], T. Kurki-Suonio[1], H. Bergsåker[2], J. Likonen[c], S. Marsen[4], C. Silva[5], S. Äkäslompolo[2] and JET EFDA contributors*

JET-EFDA, Culham Science Centre, OX14 3DB, Abingdon, UK

[1]Department of Applied Physics, Aalto University, Association Euratom-Tekes, PO Box 14100, FI-00076 AALTO, Finland
[2]KTH, Association Euratom-VR, SE-10044 Stockholm, Sweden
[3]VTT, Association Euratom-Tekes, PO Box 1000, FI-02044 VTT, Finland
[4]Max-Planck-Institute for Plasma Physics, 17491 Greifswald, Germany, EURATOM Association
[5]Associação Euratom/IST, Instituto de Plasmas e Fusão Nuclear, Instituto Superior Técnico, Portugal
** See annex of F. Romanelli et al, "Overview of JET Results", (23rd IAEA Fusion Energy Conference, Daejon, Republic of Korea (2010)).*

Preprint of Paper to be submitted for publication in Proceedings of the
20th International Conference on Plasma Surface Interactions , Eurogress, Aachen, Germany
21st May 2012 - 25th May 2012

ABSTRACT

We model the transport of a beryllium (^{10}Be) marker during a sequence of an inner-wall limited and a diverted Ohmic plasma phase in JET with the objective of identifying principal migration pathways. The 3D orbit-following code ASCOT is used for predictive analysis of an experiment during the 2011–2012 campaign on JET where three central wall tile pieces enriched with ^{10}Be were installed to an Inner Wall Guard Limiter (IWGL) of the tokamak. The simulations indicate that ^{10}Be is distributed along the IWGLs during the limiter phase which, when assuming erosion, can lead to high deposition on the inner (high-field side) divertor during the diverted phase. In contrast, beryllium penetrating into core plasma during the limiter phase is seen to be predominantly uniformly deposited during the diverted phase on the outer (low-field side) wall limiters and divertor tiles.

1. INTRODUCTION

In 2011, JET started its operation in the ITER-Like Wall (ILW) materials configuration with beryllium in the main chamber and tungsten (W) in the divertor [1]. One of the most important questions for investigation is how beryllium migrates within the main chamber, from the main chamber walls to the divertor and how the migration pattern compares to that of carbon [2]. Migration of beryllium to the divertor can potentially lead to material mixing and the build-up of Be-W layers with undesirable erosion or retention properties.

For studying beryllium migration, an isotopic marker experiment with ^{10}Be is carried out during the 2011–2012 experimental campaign on JET. Three adjacent central pieces of an inner wall guard limiter tile located poloidally above the inner midplane and toroidally in section 5Z were enriched with 10Be prior to their installation and, after shutdown, deposition of the eroded marker on selected plasma-facing components will be experimentally assessed using the Accelerator Mass Spectrometry (AMS) technique [3]. The bulk concentration of ^{10}Be in the enriched tile has been measured to be ^{10}Be/^{9}Be = 1.7×10^{-9}. The sensitivity and background level for analysis is below ^{10}Be/^{9}Be = 1.0×10^{-14}, and thus the sensitivity is sufficient to detect the marker even if it is diluted up to five orders of magnitude.

Analysis of ^{10}Be migration during the experiment is challenging for a number of reasons. As the experiment is campaign-integrated, the enriched wall tile experiences a large number of plasma discharges of different types whose cumulative effect on beryllium migration is extremely difficult to estimate. Another difficulty is due to the fact that plasma discharges in JET are predominantly inner-wall limited during the start-up phase before the X-point formation. During previous experimental campaigns with carbon walls this has been observed to constitute a major part of the inner wall erosion [4] and high sputtering yields at the IWGLs during limiter phases have been measured also during the present campaign [5]. In addition, the duration of the limiter phase (several seconds for a single discharge) is not insignificant with respect to the duration of flat top operation (up to 15 seconds).

Consequently, also the plasma start-up phase needs to be considered when analysing the migration of the marker. Apart from the experiment, impurity migration during inner-wall limited plasmas

is also of interest with respect to plasma start-up in ITER. In this contribution, 3D orbit-following simulations with the ASCOT code are carried out to investigate the global migration pathways of ^{10}Be in plasma conditions representative for the beginning of the experimental campaign.

2. MODELLING OF ^{10}BE TRANSPORT

ASCOT is a 3D Monte Carlo code for following the orbits of individual plasma particles, called test particles, on a static magnetic field and background plasma [6]. Coulomb collisions between the test particles and the background plasma are modelled using collision operators, whereas anomalous transport in the radial direction is described by a diffusion coefficient $D_\perp$. For impurities, the effective ionization and recombination of the followed particles is calculated using rate coefficients from the ADAS database [7]. Both the magnetic field and the tokamak wall geometry can be included in a three-dimensional, nonaxisymmetric form.

Here, ^{10}Be migration is studied during a sequence of two plasma scenarios that represents transition from the start-up phase into flat-top operation. The first scenario is an inner-wall limited plasma with JET Pulse Number 80836 (toroidal magnetic field $B_t = 2.5$T, plasma current $I_p = 2.5$MA, line-integrated electron density $n_e = 3.9\times10^{19}$ 1/m^3, core electron temperature $T_e = 2.1$keV) during which the dominant ^{10}Be erosion is assumed to occur, see Fig.1. The second scenario in the sequence corresponds to a diverted Ohmic plasma JET Pulse Number 80295 with $B_t = 2.0$T, $I_p = 2.0$MA, $n_e = 4.6\times10^{19}$ 1/m^3, and $T_e = 1.4$keV.

The simulation is started in the limited scenario by following an ensemble of 200 000 ^{10}Be+ test particles that are considered being eroded uniformly from the enriched IWGL tile pieces containing the ^{10}Be marker. Radially, the particles are initialized 0.19–0.24cm away from the tiles based on the ionization mean free path of the eroded Be neutrals. The test particles are given an initial energy of $E_0 = \frac{1}{2}E_B = 1.155$eV, where EB is the binding energy of beryllium [13]. As ASCOT is not capable of modelling erosion, the particles are followed until they are deposited or their maximum simulation time tmax is reached. In the limited scenario, the maximum simulation time is taken from a random uniform distribution $t_{max} \in [10^{-5}, 0.1]$s. Thus, the test particle ensemble represents ^{10}Be that is eroded during a time interval of 0.1s at the end of the inner-wall limited phase. The maximum allowed value for tmax corresponds to the time by which it was observed that a significant majority of the test particles would be deposited.

After the limited scenario, the simulation sequence is continued in the diverted scenario with using the final state of the first simulation as the initial test particle ensemble. Particles that were deposited in the limited scenario are considered being eroded and are given an initial energy of E_0. All of the test particles are given a maximum simulation time of $t_{max} = 1.0$s to avoid excessive computational time. In both scenarios, a diffusion coefficient of $D_\perp = 1.0$m^2/s is used.

During the simulations, the ^{10}Be test particles are followed on an unrestricted computational domain that extends from the core plasma through the Scrape-Off Layer (SOL) and halo plasma to the wall. For the background plasma in the core, 1D profiles of electron temperature Te and density

n_e from High-Resolution Thomson Scattering (HRTS) measurements are used for both scenarios with the assumption of equal values for background ions, i.e., $T_e = T_i$ and $n_e = n_i$.

In the limited scenario, upstream ReCiprocating Probe (RCP) measurements [8] of T_e, n_e and plasma flow velocity were utilized to create a background plasma for the SOL. Using the basic two-point model, the measured upstream values were used to calculate corresponding temperature and density values for different magnetic flux surfaces at the target locations, i.e., intersection locations with the wall, see Fig.1. For each of the flux surfaces, the temperature and density values were then calculated along the flux surface by linearly interpolating between the upstream and target values. This results in an onion-skin like plasma solution. As the plasma is in the sheath-limited regime, temperature gradients parallel to the magnetic field are in general minor and, thus, the employed approach for background plasma creation is welljustified. In a similar manner, the background plasma flow field was created based on the RCP measurements with using the Bohm criterion of Mach 1 flow velocity at the target locations as the boundary condition.

For the diverted scenario, a plasma solution calculated with the plasma fluid code EDGE2D [9] coupled to the Monte Carlo neutrals code EIRENE [10] was employed for the SOL background plasma. Plasma conditions in the halo plasma outside the EDGE2D-EIRENE computational domain were approximated with exponentially decaying profiles. The decay lengths were obtained from exponential fits to probe measurements in the far-SOL of JET Pulse No's: 81473, 81477, 81486 and 81491.

In both scenarios, a magnetic equilibrium from the EFIT code was utilized. For the simulations, a three-dimensional non-axisymmetric wall geometry of the JET ILW was created by employing a ray-tracing technique on Computer-Aided Design (CAD) data of the tokamak. Therefore, the simulations can accurately take into account the effect of, e.g., individual limiter structures on ^{10}Be transport which, in the case of ^{13}C in ASDEX Upgrade, has been observed to be of great importance for toroidal symmetry [12].

3. SIMULATION RESULTS

In the limited scenario, the SOL plasma near the inner midplane is extremely thin with a width of only a few millimeters. Consequently, the ^{10}Be ions quickly penetrate into the core plasma. For the particles that diffuse out of the confined core, the simulation shows them being strongly transported back towards the inner wall. This transport is strengthened by the high-velocity flow of the background plasma with the RCP-measured values being around Mach 0.5. In the 2D deposition profile shown in Fig.2 it can be seen that the deposited particles are both poloidally and toroidally distributed along the IGWL tiles around the torus. Although the ^{10}Be source is initially highly localized, transport in the core plasma effectively distributes the particles over different toroidal angles as they diffuse into the SOL. Poloidally, in Fig.2 the ^{10}Be deposition can be observed to be localized around two locations on most of the IWGLs, i.e, on the lower left and the upper right edges. This pattern, visualized in more detail in Fig.3, is due to the magnetic field lines that in the

vicinity of the inner midplane primarily connect to these locations on the limiters. As the ^{10}Be ions entering the SOL from the core plasma are divided into particles moving in positive and negative toroidal directions, their deposition on the IWGLs can occur on either one of these locations. The result bears resemblance to observations from experimental post-mortem studies of PFCs in JET during previous campaigns. On analysed IWGL tiles, the same locations as indicated by the simulation have been observed to be areas of net deposition [11].

Apart from the IWGLs, deposition in other regions of the wall in Fig.2 is only minor. Particles that meet their maximum simulation time before deposition (76%) were observed to remain scattered in the core plasma. Therefore, when considering ^{10}Be migration during the diverted scenario, it is noticeable that a significant fraction of the eroded ^{10}Be can exist in the core plasma before X-point formation.

When the simulation is continued in the diverted scenario, the particles that are considered being eroded from their deposition locations on the IWGL tiles are mainly either locally redeposited or being transported by the background plasma flow towards the inner divertor which leads to the strong deposition there shown in Fig.4. For particles initialized in the core plasma, it is important to notice that due to, e.g., trapped orbits, their cross-field diffusion into the SOL is strongest in the low-field side. There, the followed ^{10}Be particles are predominantly deposited on the outer poloidal limiters together with other protruding wall structures and at the outer divertor. Although plasma flow is directed towards the inner divertor across most of the SOL, it is worth noting that the particles diffusing out of the core plasma have significantly higher energies compared to their initial energy E_0 and, consequently, the effect of the flow on their transport is weaker when compared to low-energy beryllium ions.

In figure 4 it is visible that both the inner and outer divertor deposition is rather symmetric toroidally. In addition, deposition on the outer wall is rather uniformly distributed among limiters at different toroidal locations. Both of these features are explained by their origin being in the core plasma transport.

During the diverted scenario, approximately 20% of the simulated ^{10}Be was observed to still remain in the core plasma after their maximum simulation time of $t_{max} = 1.0$s. As the outflux of these particles to the SOL occurs primarily in the low-field side, their expected effect on the deposition pattern in Fig.4 is to slightly increase the deposition on the outer poloidal limiters and outer divertor. This does not, however, alter the identfied migration pathways.

In addition to the discussed migration mechanisms, the ^{10}Be particles in reality undergo further migration through an erosion-transport-deposition cycle. Long time-scale simulations of beryllium migration in JET have shown that the migration occurs in a step-wise manner towards the divertors [krieger]. In Fig.4, the erosion of ^{10}Be deposited on the outer wall can be expected due to the high particle flux experienced by the limiters. As the stagnation point of plasma flow in a lower-single null configuration is typically below the outer midplane, the migration of these particles can be directed towards both the inner and outer divertors or, as an additional possibility, towards remote

areas shadowed from direct plasma contact. Although the simulation indicates rather high ^{10}Be deposition at the outer divertor, the region has been experimentally observed to be subject to net erosion [15]. Therefore, further migration is likely to affect the simulated divertor deposition asymmetry by increasing the inner divertor deposition.

DISCUSSION AND CONCLUSIONS

Based on simulations with the ASCOT code, possible ^{10}Be migration pathways have been identified. Assuming erosion during an inner-wall limited start-up phase of a discharge, the 10Be ions are strongly penetrating into the core plasma and, when entering the SOL by crossfield transport, predominantly deposited on the most protruding inner wall guard limiters (1Z, 2X, 3X, 4X, 4Z, 5Z, 6X, 7X, 8X, 8Z) with distinct preferential deposition locations at the top and bottom parts of the limiters. In the beginning of a following diverted flat-top phase, eroded ^{10}Be can consequently be scattered around the core plasma. The diffusion from the core plasma to the SOL predominantly occurs in the low-field side which then leads to ^{10}Be deposition mainly on the outer-wall limiters and the outer divertor during the diverted operation. For ^{10}Be eroded from the IWGLs during the flat-top phase, the primary pathway is transport with the plasma flow towards the inner divertor. Both at the inner and outer divertors, 10Be deposition driven by these mechanisms is rather toroidally symmetric.

The discussed migration pathways indicate two competing mechanisms that lead to ^{10}Be deposition in the high-field and low-field sides, respectively: plasma flow driving particles most strongly towards the inner divertor and transport in the core plasma which effectively produces a particle outflux to the low-field side SOL. Regarding the simulation results, however, it should be noticed that the background plasma flow velocity calculated with EDGE2D-EIRENE is likely to be underestimated with respect to the strong flows that are in general observed. Therefore, the effect of the plasma flow on the ASCOT simulations remains correspondingly underestimated.

Furthermore, considering the implications of the presented modelling to the experimental results, it should be noted that this study focused on conditions representative of the beginning of the experimental campaign. The effect of, e.g., different plasma configurations on ^{10}Be migration remains a topic for further investigation.

ACKNOWLEDGEMENTS

This work, supported by the European Communities under the contract of Association between Euratom/Tekes, was carried out within the framework of the European Fusion Development Agreement. The views and opinions expressed herein do not necessarily reflect those of the European Commission. The supercomputing resources of CSC–IT center for science were utilized in the studies. Resources of HPC-FF are greatly acknowledged.

REFERENCES

[1]. G.F. Matthews et al., Physica Scripta **T145** (2011) 01400.

[2]. S. Brezinsek et al., Journal of Nuclear Materials **415** (2011) S936.

[3]. A. Aldahan and G. Possnert, Geophysical Research Letters **30** (2003) 1301.

[4]. A. Widdowson et al., these proceedings.

[5]. D. Borodin et al., these proceedings.

[6]. S. Sipilä, PhD Thesis, Helsinki University of Technology, 1997.

[7]. H.P. Summers, The ADAS User Manual, version 2.6 (2004), http://www.adas.ac.uk

[8]. C. Silva et al., these proceedings.

[9]. A. Taroni et al., Contribution to Plasma Physics **32** (1992) 438.

[10]. D. Reiter et al., Journal of Nuclear Materials **196–198** (1992) 80.

[11]. J.P. Coad et al., Physica Scripta **T145** (2011) 014003.

[12]. J. Miettunen et al., Nuclear Fusion **52** (2012) 032001.

[13]. Y. Kudriavtsev et al., Applied Surface Science **239** (2005) 273.

[14]. K. Krieger et al., these proceedings.

[15]. J.P. Coad et al., Nuclear Fusion **46** (2006) 350.

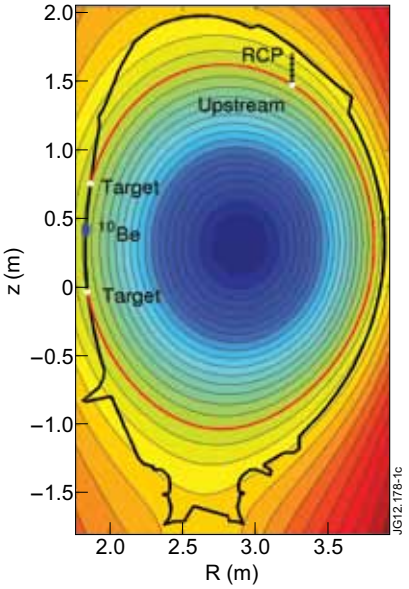

Figure 1: Magnetic flux surfaces of JET Pulse No: 80836 at 16s together with an (R,z) projection of the JET ILW geometry (black) and the location of the RCP measurements (dashed). Upstream and target locations of a single flux surface are indicated to illustrate the method used in creating the SOL background plasma for the inner-wall limited scenario of the simulated plasma sequence. The location of the 10Be marker on the IWGL is shown between the target locations.

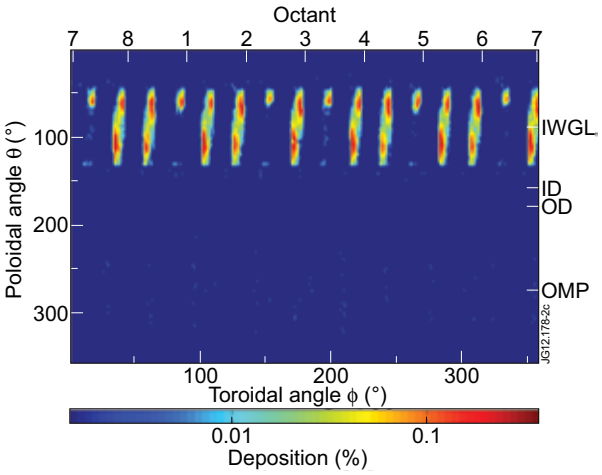

Figure 2: Deposition pattern of 10Be simulated with ASCOT during the inner-wall limited plasma JET Pulse No: 80836. The percentages indicate deposition relative to the total number of deposited particles. The poloidal angle starts from the top of the vessel increasing towards the inner wall as indicated by the labels IWGL, ID, OD and OMP for the inner-wall guard limiters, inner and outer divertors and outer midplane, respectively.

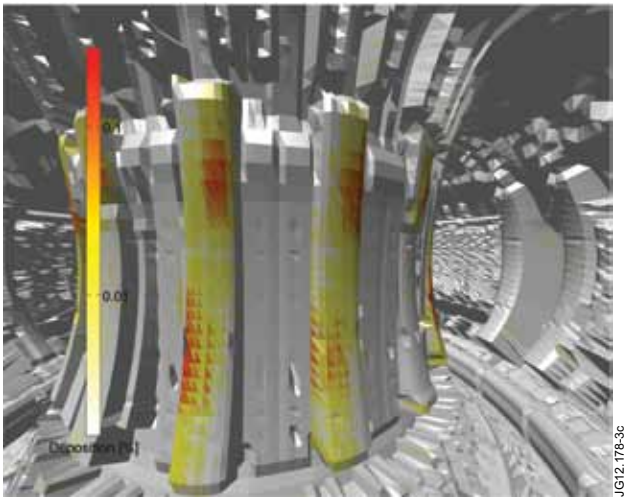

Figure 3: Visualization of the 10Be deposition on the inner wall guard limiters around octant 4 during the inner-wall limited plasma phase together with the 3D wall geometry used in the simulations. Deposition is clearly preferential on the top and bottom parts of the limiters. Notice the logarithmic scale.

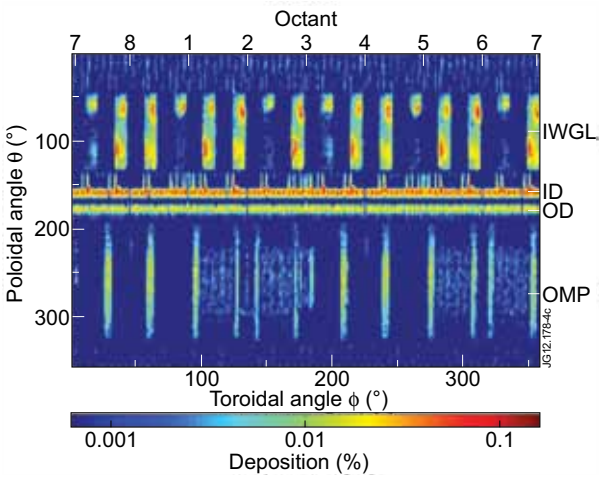

Figure 4: Deposition pattern of ^{10}Be as the simulation sequence is continued in the diverted plasma JET Pulse No: 80295. The labels are the same as in Fig.1.